

PHYSICAL AND MATHEMATICAL MODELLING OF IGNITION OF SMALL MAGNESIUM PARTICLES

Fedorov A.V. *, Shulgin A.V. and Tropin D.A.

*Author for correspondence

Khristianovich Institute of Theoretical and Applied Mechanics
of the Siberian Branch of the Russian Academy of Sciences,
Institutskaya street, 4/1, Novosibirsk, 630090,
Russia

E-mail: fedorov@itam.nsc.ru

ABSTRACT

The distributed mathematical model (nonstationary 1D and 2D) of magnesium particle ignition is developed taking into account the heterogeneous chemical reaction, the domain of particle thermal influence to gas, and the realistic particle temperature after ignition. Solvability of the corresponding mathematical problem in the stationary one-dimensional case in some kinds of symmetry has allowed one to expand classification of regular modes of heating, and also modes of extinction and ignition of a particle. The numerical method for solving the considered class of boundary value problems of magnesium particles ignition is developed, and the mathematical model is verified by the experimental dependences of: ignition delay time on surrounding gas pressure and particle radius; limiting ignition gas temperature on surrounding gas pressure and particle radius. The limiting size of a gas layer near a particle is found that determines an ignition mode in the frame of this realistic mathematical model.

The work was supported financially by the Russian Foundation for Basic Research, Grant No 06-01-00299.

INTRODUCTION

The problem of physical and mathematical modelling of ignition and combustion of metal samples is of considerable interest for various branches of industry [1-4]. The work [3] mainly presented the pointwise and partially distributed models of the process of fine metal particles ignition, when the low-temperature oxidation process occurred on the particle surface. The heat diffusion into the gaseous phase was not taken into account therein. This means that the so-called "reduced film" has a negligibly small thickness. It appears to be of interest to study the influence of the given factor on thermal history of the reacting particle. In the present work, the results obtained in [5] are extended for the case of a mathematical model enabling the obtaining of a realistic particle temperature after its ignition.

This is due to the use of concepts on the deceleration of part of heterogeneous reactions occurring on the particle surface upon reaching some limiting temperature T_m . The influence of thermal field inhomogeneity on the heating and ignition of the magnesium particle is also investigated.

PHYSICAL AND MATHEMATICAL PROBLEM FORMULATION

One-dimensional problem

Consider the problem of ignition of magnesium samples covered by an oxide layer. As such samples, a magnesium plate, a cylindrical thread, and a spherically symmetric particle were taken with typical sizes $r_p = 15 \div 60 \mu\text{m}$ surrounded by a gas layer with thickness $L - r_p$. Assume that an exothermal chemical reaction of oxidation occurs on the sample surface. The mathematical model describing the temperature fields of particle T_2 and the ambient gas T_1 then has the form

$$\rho_2 c_2 \frac{\partial T_2}{\partial t} = \lambda_2 \frac{1}{r^\nu} \frac{\partial}{\partial r} \left(r^\nu \frac{\partial T_2}{\partial r} \right), \quad 0 \leq r \leq r_p, \quad (1)$$

$$\rho_1 c_1 \frac{\partial T_1}{\partial t} = \lambda_1 \frac{1}{r^\nu} \frac{\partial}{\partial r} \left(r^\nu \frac{\partial T_1}{\partial r} \right), \quad r_p \leq r \leq L, \quad (2)$$

where ν is the symmetry exponent equal to 0, 1, and 2 for the Cartesian, polar, and spherical coordinates, respectively, $\rho_i, \lambda_i, c_i, i = 1, 2$ are the densities, the thermal conductivities, and the specific heats of phases, the subscripts 1 and 2 refer to the parameters of gas and particle. Equations (1) and (2) must satisfy the following initial conditions:

$$t = 0: T_2(r) = T_1(r) = T_0 \quad (3)$$

and boundary conditions

$$\begin{aligned} r = 0: \quad \partial T_2 / \partial r = 0, \quad r = L: \quad \lambda_1 \partial T_1 / \partial r = -\alpha (T_1 - T_c), \\ r = r_p: \quad T_1 = T_2, \quad \lambda_1 \partial T_1 / \partial r + q_0 \rho_3 dh/dt = \lambda_2 \partial T_2 / \partial r. \end{aligned} \quad (4)$$

Here $q_0, \rho_3, h, dh/dt = f(T_m, T_2) K \exp[-E/(RT_2)]$, $K, E, R, \alpha = \text{Nu}/2$, Nu, T_c are the specific heat release per a unit oxide mass, the oxide density, the oxide film thickness, the rate of the oxide film thickness variation, the pre-exponent in the oxidation law, the activation energy of low-temperature oxidation, the universal gas constant, the heat transfer coefficient, the Nusselt number, and the temperature at the gaseous region boundary. Functions $f(T_m, T_2) = 1$ (model 1) or $f(T_m, T_2) = T_m - T_2$ (model 2) describe the chemical reaction type. The function $h(t)$ describes the temporal dependence of the oxide film thickness, and the oxidation problem (1), (2) must generally be posed as a free boundary problem. The oxide film thickness, however, varies very weakly during the pre-ignition period, which enables a problem splitting so that it is possible to set a boundary condition describing the oxidation at the particle boundary.

Let us introduce the dimensionless variables and parameters by the formulas

$$\begin{aligned} \bar{r} = r/r_p, \quad \bar{L} = L/r_p, \quad \bar{T}_i = T_i/T_0, \quad \bar{t} = t/t_0, \quad t_0 = \rho_2 c_2 r_p^2 / \lambda_2, \\ \bar{\alpha} = r_p \alpha / \lambda_1, \quad \bar{q}_0 = q_0 \rho_3 K r_p / (\lambda_1 T_0), \quad \bar{E} = E/RT_0, \\ \bar{\lambda} = \lambda_2 / \lambda_1, \quad \bar{C}_1 = (\lambda_1 \rho_2 c_2) / (\lambda_2 \rho_1 c_1). \end{aligned}$$

Relations (1)–(4) then take the following form:

$$\frac{\partial \bar{T}_2}{\partial \bar{t}} = \frac{1}{\bar{r}^\nu} \frac{\partial}{\partial \bar{r}} \left(\bar{r}^\nu \frac{\partial \bar{T}_2}{\partial \bar{r}} \right), \quad 0 \leq \bar{r} \leq 1, \quad (5)$$

$$\frac{\partial \bar{T}_1}{\partial \bar{t}} = \frac{\bar{C}_1}{\bar{r}^\nu} \frac{\partial}{\partial \bar{r}} \left(\bar{r}^\nu \frac{\partial \bar{T}_1}{\partial \bar{r}} \right), \quad 1 \leq \bar{r} \leq \bar{L}, \quad (6)$$

$$\bar{t} = 0: \quad \bar{T}_2(\bar{r}) = \bar{T}_1(\bar{r}) = 1, \quad (7)$$

$$\bar{r} = 0: \quad \partial \bar{T}_2 / \partial \bar{r} = 0, \quad \bar{r} = \bar{L}: \quad \partial \bar{T}_1 / \partial \bar{r} = -\bar{\alpha} (\bar{T}_1 - \bar{T}_c),$$

$$\bar{\lambda} \partial \bar{T}_2 / \partial \bar{r} = \partial \bar{T}_1 / \partial \bar{r} + \bar{q}_0 \bar{f}(\bar{T}_m, \bar{T}_2) \exp(-\bar{E}/\bar{T}_2), \quad (8)$$

where $\bar{f}(\bar{T}_m, \bar{T}_2) = 1$ (model 1) or $\bar{f}(\bar{T}_m, \bar{T}_2) = \bar{T}_m - \bar{T}_2$ (model 2). The bars over the variables will be omitted in the following that is all the quantities of the mathematical model will be assumed to be dimensionless henceforth.

Two-dimensional problem

We consider in the following a two-phase medium consisting of magnesium particles of radius r_p , $R_p = \{-r_p \leq x, y \leq r_p\}$, which lies in the rectangular gaseous region $R_g = \{(x, y) \in (-L_x, L_x) \cup (-L_y, L_y) \setminus R_p\}$ (Figure 1). In dimensionless variables, which are introduced similarly to

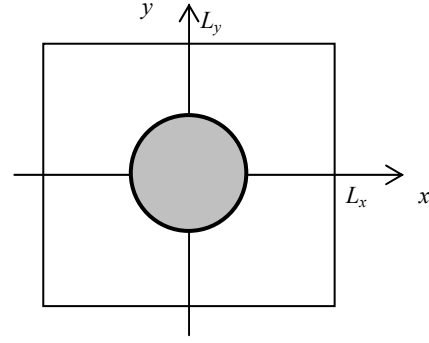


Figure 1 Gas — particle system

the way described above, the temperature field of the system is described by the heat equation

$$\frac{\partial T}{\partial t} + \text{div}(-k \nabla T) = 0 \quad (9)$$

under the initial condition

$$T(x, y, 0) = T_0(x, y, 0), \quad (10)$$

the heat exchange condition on the gaseous region boundary $(x, y) \in \partial R_g$

$$\nabla T(x, y, t) = -\alpha (T(x, y, t) - T_c(x, y)), \quad (11)$$

and the boundary condition at the interface of phases $(x, y) \in \partial R_p$

$$\lambda \nabla T_+ = \nabla T_- + q_0 f(T_m, T_2) \exp(-E/T). \quad (12)$$

Here $k = 1$ in the particle region, $k = C_1$ in the gas region, and the “+” and “-” signs mean the value at the interface on the particle and gas side, respectively.

STEADY APPROXIMATION

We recall that, as was found previously in [3, 5] from the elementary catastrophe theory in the one-dimensional formulation, we have a nonlinear equation for the stationary temperature value T_2 of the sample, which has two roots

$$T_2^\pm = \frac{E}{2} \left(1 \pm \sqrt{1 - \frac{4T_c}{E}} \right) \quad (13)$$

for model 1 and

$$T_2^\pm = \frac{E(T_m + T_c)}{2(E + T_m - T_c)} \left[1 \pm \sqrt{1 - \frac{4T_m T_c (E + T_m - T_c)}{E(T_m + T_c)^2}} \right] \quad (14)$$

for model 2. The manifold of catastrophes/ignitions itself is determined by relations

$$\beta = \frac{\alpha L^\nu / q_0}{1 + \alpha L(1 - L^{\nu-1}) / (\nu - 1)} = \frac{f(T_m, T_2)}{T_2 - T_c} \exp\left(-\frac{E}{T_2}\right) \quad (15)$$

for $\nu = 0, 2$, and

$$\beta = \frac{\alpha L / q_0}{1 + \alpha L \ln L} = \frac{f(T_m, T_2) \exp(-E/T_2)}{T_2 - T_c} \quad (16)$$

for $\nu = 1$. The given manifold represents an S-shaped curve in the (β, T_2) plane, where T_2 is the sample temperature after the reaction termination, and has two turning points with coordinates (β_{\pm}, T_2^{\pm}) , where the β_{\pm} values are calculated by formulas (15), (16) with the T_2 value determined by relations (13) and (14). This curve is universal for all three samples. The differences manifest themselves only at a passage to the β, T_2 values. The given manifold has three branches, which determine the types of thermal dynamics of the sample: at $\beta \geq \beta_+$ the solution $T_2 \in [T_-, T_c]$ and describes the regime of regular heating; at $\beta_- \leq \beta \leq \beta_+$, we have $T_2 \in [T_-, T_+]$, which corresponds to an unstable heating regime; at $0 \leq \beta \leq \beta_-$, $T_2 \geq T_-$, and the solution gets on the branch of the manifold of ignitions, which corresponds to the phenomenological ignition criterion.

DISCUSSION OF COMPUTATIONAL RESULTS

We will consider in the following only such a type of the particle thermal dynamics as ignition. In this case, the determination of experimentally observed quantities: the ignition delay time and the limiting temperature of the sample ignition proves to be useful. We now present the results of the computation of the one-dimensional problem by model 2 by the numerical method developed previously by the authors of [5].

Ignition delay time

Let us go over to the analysis of the first experimentally observed parameter — the ignition delay time depending on the problem symmetry. Figure 2 shows the graphs of the ignition delay time versus the sample reference size for all three symmetry kinds of samples for the dimensionless value $L = 2$.

Each graph presents the curves for different values of the ambient gas temperature. It is seen that the ignition delay time drops with reducing radius and increasing temperature of the ambient gas.

These dependencies are interrupted at some points. This points to the fact that the ignition will not occur for the given ambient gas temperature with reducing particle size. And for this particle size, at which the graph interrupts, the gas temperature will be limiting. It is also seen that the limiting temperature will grow with decreasing size. This temperature growth will be explained below, where we consider the limiting ignition temperature.

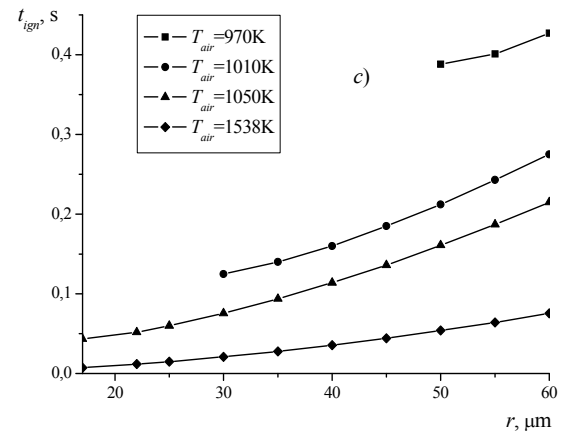
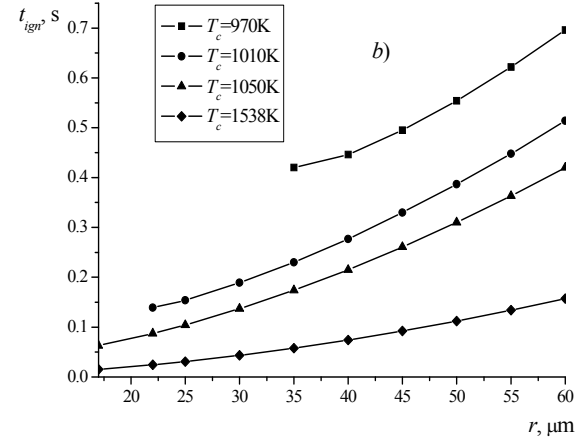
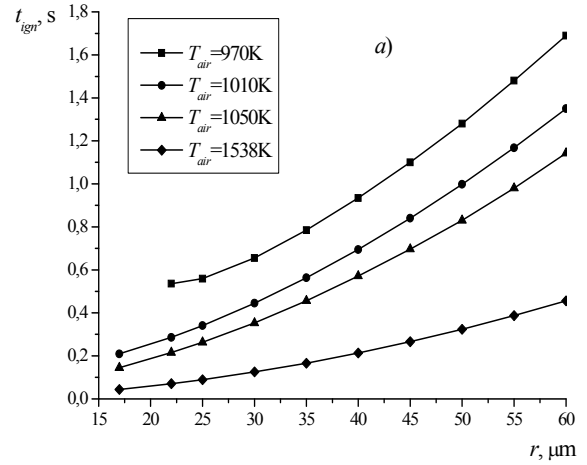


Figure 2 Ignition delay time of the particle vs. its size. Fine particles, a) plate, b) thread, c) spherical particle

Limiting ignition temperature

Let us go over to the description of the second experimentally observed parameter — the limiting ignition temperature depending on the particle radius variation. The limiting ignition temperature is known to be the minimum temperature of the ambient gas at which the ignition is still possible.

Figure 3 shows the limiting ignition temperature depending on the sample size. The experimental dependence was taken from [6], where to determine the ignition temperature of spherical magnesium particles a Vycor tube contained in vertical Nichrome furnace was filled with dry air. Magnesium particles were dropped through a water-cooled inlet into the furnace and heated. A comparison of computed and experimental data shows that the computed data describe satisfactorily the experimental data within the given range of particle sizes (15–90 μm).

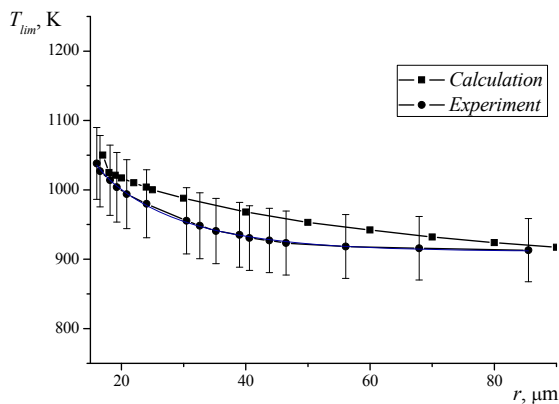


Figure 3 Limiting ignition temperature. Computed and experimental data

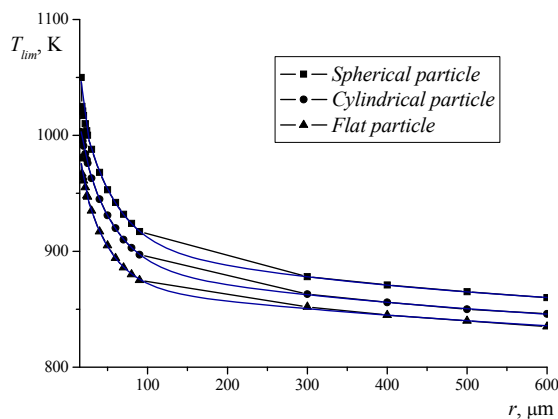


Figure 4 Generalized characteristic

Figure 4 shows the generalized characteristic in the form of the limiting ignition temperature dependence of the particle size for sizes from 15 to 600 μm and for all three sample kinds. It is

seen from this dependence that the limiting ignition temperature increases with reducing radius. This is explained as follows. The particle is heated fairly quickly up to the ambient gas temperature. A further heating is due to a higher heat supply to the particle at the expense of chemical reaction as compared to the heat removal into the environment. A reduction of the particles size leads to an increase in the heat-transfer coefficient, which accelerates the particle heating at the initial stage and slows down at the final stage. Accounting for an insignificant duration of the initial stage as compared to the entire heating time we obtain that a higher environmental temperature than for large particles is needed for fine particles.

The ambient pressure influence

It appears interesting to extend the region of the particle ignition description depending on model parameters versus the gas pressure. Let the pre-exponent in the oxidation law depend linearly on pressure: $K(P) = 0.0146 + 0.0774 \cdot P$. The limiting temperature was plotted for the function $K(P)$ determined in this way versus the particle size for various ambient gas pressures (Figure 5).

The computed limiting temperature can be seen to drop with increasing pressure. At the ignition instant, the heat supply to the particle at the expense of chemical reaction must be close to the heat removal into the environment. Since the particle temperature at the ignition instant depends weakly on the variation of medium parameters, the pressure increase leads to an increase in heat release at the expense of pre-flame chemical reactions, which cause a reduction of the limiting ignition temperature [7].

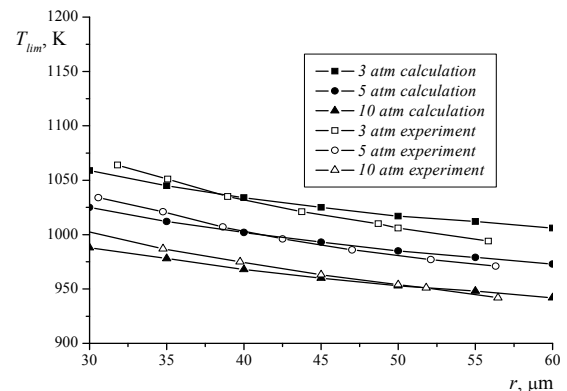


Figure 5 Limiting ignition temperature vs. the radius and ambient pressure

Two-dimensional problem

The problem was solved in the two-dimensional formulation with the aid of the FlexPDE package [8]. For the assessment of results obtained with the aid of using the FlexPDE package the test computations were executed for comparison with the data of [5] obtained by the method developed on the basis of the Thomas algorithm in the one-dimensional statement. We assume to this end that the gaseous

region R_g represents an annulus at the boundary of which the uniform heat exchange condition (11) is specified. The task was solved by the method of [5] in the one-dimensional statement by virtue of its symmetry, and this task was solved with the aid of FlexPDE as a two-dimensional task. Table 1 presents the ignition time t_{ign} versus the gaseous region size L , which was obtained by the Thomas algorithm (columns 1–3) and by FlexPDE (column 4).

L	t_{ign} , ms			
	Model 1	Model 2		
2	20.9	21.6	18.4	21
4	23.2	23.4	19.8	23.2
6	24.6	24.8	21.2	24.55
8	25.2	25.8	22	25.6
10	25.6	26.5	22.7	26.4

Table 1

The data presented in columns 2, 3, 4, and 5 were obtained by model 1 [5], by model 2 for $\beta = 7.09181 \cdot 10^{-5} < \beta_-$, by model 2 for $\beta = 1.05600 \cdot 10^{-5} < \beta_-$, and by model 2, respectively.

The ignition time is presented in Table 2 versus the particle radius by model 2 for the values $\beta = 1.05600 \cdot 10^{-5}$, $L = 2$, $T_c = 1122$ K, and $T_c = 1538$ K. Computation by the method of [5] (columns 1 and 2) and by FlexPDE (columns 3 and 4).

The ignition delay time increases with increasing particle radius. And it drops at a fixed radius and increasing ambient temperature, as this was to be expected.

r_p , μm	t_{ign} , ms			
	Method [5]		FlexPDE	
	$T_c = 1122$ K	$T_c = 1538$ K	$T_c = 1122$ K	$T_c = 1538$ K
17	21.6	8.5	21	7.9
20	29.9	11.78	29.2	11.2
30	67.4	26.5	66.8	26
40	119.7	47.1	119.1	46.6
50	187.1	73.6	186.7	73.2
60	269.4	106	268.6	105.4

Table 2

The agreement in results on the ignition delay times obtained by computations using different models and different numerical procedures can be seen to be quite satisfactory: the maximum difference does not exceed 2%.

Let the gas region R_g now represent a square with sides $L_x = L_y = 2$, and the particle lies at the center of the region under consideration. For the particle of radius $r_p = 17$ μm and the temperature $T_c = 1122$ K at the gaseous region boundary,

the ignition delay time of 21 ms was obtained by the computation using the one-dimensional model, whereas the time of 21.5 ms was obtained by the computation using the two-dimensional model (for the annular gas region surrounding the particle the temporal difference in the ignition delay time amounted to about 2%) and of 23.5 ms (for a square gas region surrounding the particle the temporal difference in the ignition delay time amounted to about 11%). The gaseous region area increased by 25%. An increase in the ignition delay time when passing to a square region from an annular one may physically be explained by an increase in the ambient gas volume, which leads to the need in a longer heating.

Now consider the non-uniform heating case. Let the boundary conditions at the gaseous region boundary have the following form:

$$\nabla T(\pm L_x, y, t) = -\alpha(T(\pm L_x, y, t) - T_c), \quad -L_y \leq y \leq L_y,$$

$$\nabla T(x, \pm L_y, t) = -\alpha(T(x, \pm L_y, t) - T_{c1}), \quad -L_x \leq x \leq L_x,$$

where the medium temperature at vertical boundaries of the gaseous region took the values $T_c = 1122, 1300, 1500$ K, and the temperature values T_{c1} on horizontal boundaries of the gaseous region were chosen to be lower than the critical ignition temperature T_{cr} , which in the case under consideration amounts to about 950 K [5]. Figure 6 shows the ignition delay time as the T_{c1} value drops on horizontal boundaries of the square gas region with $L_x = L_y = 2$. As follows from presented data, with decreasing T_{c1} values, an increase in the ignition delay time occurs, and no ignition occurs when T_{c1} reaches some minimum value (600, 400, and 200 K, respectively, in considered variants), and a regular heating regime takes place.

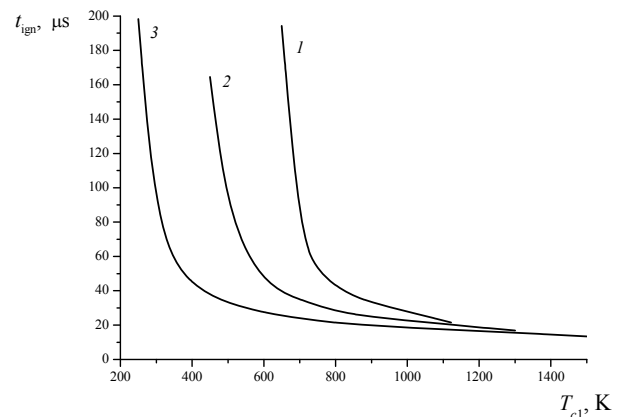


Figure 6 The ignition delay time at a reduction of the T_{c1} value: $T_c = 1122$ K — curve 1, $T_c = 1300$ K — curve 2, $T_c = 1500$ K — curve 3

Let us introduce the concept of the averaged temperature of the gaseous region boundary $T_{av} = \sum_i S_i T_{ci} / \sum_i S_i$, where T_{ci} is the temperature value at the i -th boundary, S_i is the area of the i -th boundary. As follows from the presented computations, the ignition condition is $T_{av} > 875$ K in all three variants. This value agrees with the accuracy of about 8 % with the value of the ignition critical temperature T_{cr} . Thus, the averaged temperature T_{av} may serve an ignition criterion, namely, the particle ignition will take place, if $T_{av} \gtrsim T_{cr}$.

CONCLUSION

To describe the thermal history of the magnesium particle surrounded by gaseous atmosphere the distributed mathematical nonstationary 1D- and 2D-models have been proposed, which account for the heterogeneous chemical reaction and the region of the particle thermal influence on the gas.

These models were verified in terms of the ignition delay time versus the gas pressure and radius and the limiting temperature vs. the particle radius and the ambient gas pressure.

In the case of a non-uniform heating of particles, it proved possible to substantiate the concept of the limiting temperature of particle ignition.

REFERENCES

- [1] Brooks K.P, and Beckstead M.W., Dynamics of aluminium combustion, *Journal of Propulsion and Power*, Vol. 11, No 4, 1995, pp. 769-780
- [2] Chen Z., and Fan B, Flame propagation through aluminium particle cloud in combustion tube, *Journal of Loss Prevention in the Process Industries*, Vol. 18, 2005, pp. 13-19
- [3] Fedorov A.V., Fomin V.M., and Gosteev Yu.A., Theoretical Description of the Ignition of Reacting Gas-Particle Mixtures. Published by the Novosibirsk State Univ. Civil Engng., Novosibirsk, 2003., p.
- [4] Khaikin B.I., Bloshenko V.N., and Merzhanov A.G, On ignition of metal particles, *Combustion, Explosion and Shock Waves*, Vol. 6, 1970, pp. 474-488
- [5] Fedorov A.V., and Shulgin A.V., Conjugate mathematical model of ignition of magnesium samples, *Combustion, Explosion and Shock Waves*, Vol. 42, No. 3, 2006, pp. 295-301
- [6] Cassel H.M., and Liebman I., Combustion of Magnesium particles – 2. Ignition Temperatures and Thermal Conductivities of Ambient Atmospheres, *Combustion and Flame*, Vol. 7, No 1, 1963, pp. 79-81
- [7] Kudryavtsev V.M., Sukhov A.V., and Voronetskii A.V., Investigation of the ignition of magnesium particles in air, *Izvestiya VUZov, Mashinostroenie*, No 5, 1977, pp. 81-84 (in Russian)
- [8] <http://www.pdesolutions.com>